OPTIMIZATION OF VIRUS-INDUCED GENE SILENCING TO FACILITATE EVO-DEVO STUDIES IN THE EMERGING MODEL SPECIES *MIMULUS GUTTATUS* (PHRYMACEAE)[1]

Jill C. Preston,[2] *Laryssa L. Barnett,*[2,3] *Matthew A. Kost,*[2,4] *Nathan J. Oborny,*[2,5] *and Lena C. Hileman*[2,6]

ABSTRACT

Mimulus guttatus DC. (yellow monkey-flower; Phrymaceae) is an important model species for ecological and evolutionary studies, being locally adapted to a wide range of elevation, moisture and temperature gradients, soil types, and pollinator availabilities. In order to advance this species as a model for evolutionary genetic studies, we have developed virus-induced gene silencing (VIGS) using the tobacco rattle virus (TRV) to assay gene function. We demonstrate the effectiveness of *Agrobacterium*-mediated VIGS in two divergent populations of *M. guttatus*, Iron Mountain 767 (IM767) and Point Reyes (PR). Plants infected with a fragment of the carotenoid biosynthesis pathway gene *PHYTOENE DESATURASE* (*PDS*) cloned into the TRV2 vector exhibited endogenous *PDS* silencing and photobleached phenotypes. We further assayed for VIGS-induced floral phenotypes by silencing paralogous genes putatively affecting floral symmetry, *CYCLOIDEA1* (*CYC1*) and *CYCLOIDEA2* (*CYC2*). Simultaneous silencing of *CYC1* and *CYC2* resulted in organ number defects in the petal and stamen whorls; silencing of *CYC1* affected petal margin growth; and silencing of *CYC2* had no effect on flower development. Infection with TRV2 and TRV1 is significantly higher and more pervasive in the IM767 versus the PR population and is more efficient after vacuum infiltration. These results demonstrate the efficacy of VIGS for determining the function of developmental genes, including those involved in ecologically important reproductive traits.

Key words: *CYCLOIDEA*, *Mimulus*, Phrymaceae, *PHYTOENE DESATURASE* (*PDS*), reverse genetics, virus-induced gene silencing (VIGS).

The cosmopolitan plant genus *Mimulus* L. (Phrymaceae) comprises ca. 160 to 200 species, the majority of which are derived from two rapid radiations in western North America and Australia (Beardsley & Olmstead, 2002). Species of *Mimulus* occupy a vast range of habitats, from desert to alpine, and are phenotypically diverse in both reproductive and life history traits (Vickery, 1978; Beardsley et al., 2004; Angert & Schemske, 2005; Wu et al., 2008). For example, major differences in floral form are associated with multiple shifts in pollinators and changes in the relative importance of selfing versus outcrossing (Bradshaw & Schemske, 2003). Much of the ecological and morphological diversity within the genus is evident in the young, but genetically diverse, species complex *M. guttatus* DC. (yellow monkey-flower) (Kelly & Willis, 1998; Sweigart & Willis, 2003; Beardsley et al., 2004). Populations of the *M. guttatus* complex are locally adapted to a range of elevation, moisture and temperature gradients, soil types, and pollinator availability, making them an excellent system for ecological studies (Allen & Sheppard, 1971; Fishman et al., 2002; Hall & Willis, 2005; Wu et al., 2008). Recent development of genomic tools, including a near-complete genome sequence of *M. guttatus*, have further made *Mimulus* an exciting model group in which to test fundamental evolutionary questions related to speciation, adaptation, and macroevolution (Hall & Willis, 2006; Holeski & Kelly, 2006; Cooley & Willis, 2009; Ivey et al., 2009; Lowry et al., 2009; Wu et al., 2010).

In addition to genomic tools, the development of *Mimulus guttatus* for evolutionary developmental genetic ("evo-devo") studies requires transformational capabilities to assay gene function. This can either be accomplished through forward or reverse genetic

[1] *Mimulus guttatus* DC. seeds and TRV vectors were provided by J. K. Kelly at the University of Kansas and S. P. Dinesh-Kumar at the University of California, Davis, respectively. This work was supported by a National Science Foundation grant (IOS-0616025) to L. C. H.

[2] University of Kansas, Ecology and Evolutionary Biology, 1200 Sunnyside Avenue, Lawrence, Kansas 66045, U.S.A.

[3] Current address: Duke University, Department of Biology, Durham, North Carolina 27708, U.S.A. LLB22@duke.edu.

[4] Current address: Ohio State University, Horticulture and Crop Science, Columbus, Ohio 43210, U.S.A. matthew.kost@gmail.com.

[5] Current address: University of Kansas, Department of Chemistry, Lawrence, Kansas 66045, U.S.A. noborny@ku.edu.

[6] lhileman@ku.edu.

doi: 10.3417/2010120

approaches. One promising reverse genetic method for the rapid and transient (intragenerational) silencing of gene expression is virus-induced gene silencing (VIGS) (Baulcombe, 1999; Robertson, 2004; Purkayastha & Dasgupta, 2009; reviewed in Di Stilio, 2011). VIGS utilizes the RNA interference (RNAi) pathway of plants to target endogenous messenger RNA (mRNA) for degradation (Fagard & Vaucheret, 2000; Robertson, 2004). Specifically, *Agrobacterium*-mediated infection of plant cells with a modified viral vector, containing a plant gene of interest, results in the expression of double-stranded RNAs that are degraded in vivo by DICER-like enzymes (Hamilton & Baulcombe, 1999; Zamore et al., 2000). This results in short, interfering RNAs of 12 to 23 bp that form the template for further degradation of complimentary RNAs, including endogenous mRNAs (Hammond et al., 2000; Zamore et al., 2000).

VIGS has proven effective in a wide range of distantly related angiosperm taxa (Di Stilio, 2011), including the monocots *Brachypodium distachyon* (L.) P. Beauv. (purple false brome) (Demircan & Akkaya, 2010), *Hordeum vulgare* L. (barley) (Holzberg et al., 2002), orchids (Lu et al., 2007), *Triticum aestivum* L. (wheat) (Scofield et al., 2005; Tai et al., 2005; Scofield & Nelson, 2009), and *Zingiber officinale* Roscoe (culinary ginger) (Renner et al., 2009); the basal eudicots *Aquilegia vulgaris* L. (common columbine) (Gould & Kramer, 2007), *Eschscholzia californica* Cham. (California poppy) (Wege et al., 2007), *Papaver somniferum* L. (opium poppy) (Hileman et al., 2005), and *Thalictrum* sp. L. (meadow rue) (Di Stilio et al., 2010); the asterids *Antirrhinum majus* L. (snapdragon) (Preston & Hileman, 2010), *Nicotiana benthamiana* Domin (tobacco) (Kumagai et al., 1995), *Petunia hybrida* (Hook.) Vilm (petunia) (Spitzer et al., 2007), *Solanum lycopersicum* L. (tomato) (Liu et al., 2002), and *Spinacia oleracea* L. (spinach) (Sather et al., 2010); and the rosids *Arabidopsis thaliana* (L.) Heynh. (thale cress) (Burch-Smith et al., 2006; Pflieger et al., 2008; Igarashi et al., 2009), *Glycine max* (L.) Merr. (soybean) (Zhang et al., 2009), and *Medicago truncatula* Gaertn. (Grønlund et al., 2008). However, despite the generality of VIGS, it is clear that not all vectors are effective in all species and that protocol optimization is required to elicit efficient gene silencing in nonmodel taxa (Liu & Page, 2008; Di Stilio, 2011).

Here, we demonstrate the effective use of VIGS in two morphologically diverse populations, Point Reyes (PR) and Iron Mountain 767 (IM767), of the emerging model species *Mimulus guttatus* using constructs containing *PHYTOENE DESATURASE* (*PDS*) or paralogous *CYCLOIDEA*-like (*CYC*-like) genes. *PDS* is a functionally conserved plant gene that is involved in the carotenoid biosynthesis pathway that protects the chloroplast from photo-oxidation; *PDS* silencing causes a characteristic photobleaching phenotype under high light growth conditions (Demmig-Adams & Adams, 1992; Benedito et al., 2004; Hileman et al., 2005; Gould & Kramer, 2007). By contrast, *CYC*-like genes generally affect cell proliferation and expansion in the petal and stamen whorls, mainly in the dorsal region of the flower (Luo et al., 1996, 1999; Cubas et al., 1999; Feng et al., 2006; Busch & Zachgo, 2007; Broholm et al., 2008; Fambrini et al., 2011).

Materials and Methods

Construction of *Mimulus guttatus* TRV2 VIGS vector

RNA was extracted from *Mimulus guttatus* PR and IM767 material using the RNeasy Plant Mini Kit and RNase-Free DNase Set (Qiagen, Valencia, California), and complementary DNA (cDNA) was generated using the iScript cDNA Synthesis Kit (Bio-Rad, Hercules, California). *MgPDS* was amplified from cDNA of both *M. guttatus* populations using the conserved primers ALL.PDS-F (5′-TTGWATGCCAARYAARCCWG-3′) and ALL.PDS-R (5′-ACACTIAGMAGKGRRCTTCTGC-3′), which carry degeneracies in order to amplify *PDS* from a number of taxa in the Lamiales. *MgCYC1* and *MgCYC2* were amplified from IM767 cDNA using the primers MgCYC1.full.F (5′-ACATGATTCCTCATGGCTCTTCTC-3′) and MgCYC1.full.R (5′-ACTTGTGGTGATCCAAAATGGCAG-3′), and MgCYC2.full.F (5′-CAGTTACCTCCATCCTCAGGCAAC-3′) and MgCYC2.full.R (5′-ACTTGTGCTGGTCCAAAATAGCAC-3′). The resulting fragments were cloned separately into TOPO-TA 2.1 (Invitrogen, Carlsbad, California), and their identity was confirmed by sequencing with reference to the published genome sequence (<http://www.phytozome.net/mimulus>). Nested fragments of *MgPDS* (Fig. 1), *MgCYC1*, and *MgCYC2* were amplified with primers PDS-F-BamHI (5′-ATAGGATCCTTGCWATGCCAARYAARCCWGG-3′) and PDS-R-XhoI (5′-AGTCTCGAGACACTIAGMAGKGRRCTTCTGC-3′), MgCYC1.VIGS.BamHIF (5′-ATAGGATCCGCAGCAAAGTAATAACCCTTCG-3′) and MgCYC1.VIGS.XhoIR (5′-AGTCTCGAGTCCTTCGAACCAGCTCCTTTAC-3′), and MgCYC2.VIGS.KpnIF (5′-AGTGGTACCCGGCATTGCTAGAAAGTTCTTC-3′) and MgCYC2.full.R to generate 5′ and 3′ restriction enzyme recognition sites. The resulting polymerase chain reaction (PCR)

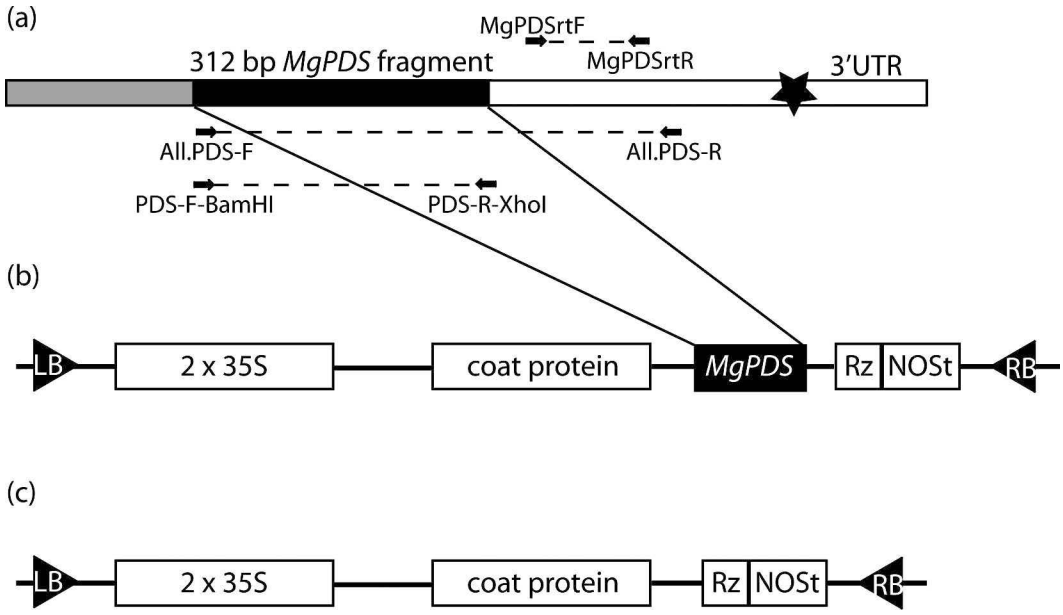

Figure 1. Example VIGS constructs. —A. Structure of *MgPDS* showing the 312 bp fragment (black) cloned into TRV2, the 5′ (gray) and 3′ (white) ends, and the position of the stop codon (star). Primer pairs used for amplification and sequencing are shown with arrows and dashed lines. —B. Map of the *MgPDS*-TRV2 construct used for VIGS. —C. Map of the Empty-TRV2 construct used as an experimental control. LB, left border; RB, right border; Rz, self-cleaving ribozyme; NOSt, NOS terminator.

fragments were digested with *Bam*HI and *Xho*I (*PDS* and *MgCYC1*), or *Kpn*I and *Xho*I (*MgCYC2*) and subcloned individually or together (*MgCYC1* and *MgCYC2*) into the tobacco rattle virus 2 (TRV2) vector digested with the same enzymes (Fig. 1).

ELECTROPORATION OF *AGROBACTERIUM TUMEFACIENS* WITH MODIFIED TRV2

To optimize infection of *Mimulus guttatus*, *MgPDS*-TRV2, or Empty-TRV2, and TRV1 were used to electroporate two strains of *Agrobacterium tumefaciens* Smith & Townsen (GV3101 and EHA105) (Dinesh-Kumar et al., 2003; Hileman et al., 2005). *Agrobacterium tumefaciens* was prepared according to a modified protocol (Hileman et al., 2005). Single colonies were used to inoculate 5 mL Luria Broth (LB) and were screened for the presence of the appropriate plasmids using primers pYL156F/pYL156R (TRV2 constructs) and OYL195/OYL198 (TRV1) as previously described (Hileman et al., 2005). PCR-positive cultures were used to inoculate 500 mL LB and were grown to an absorbance at 260 nm (Abs_{260}) of seven to nine. Pelleted cultures were resuspended in infiltration media (Hileman et al., 2005) to a final Abs_{260} of two, incubated for four to 12 hr. at room temperature, and used to inoculate *M. guttatus* PR and IM767 seedlings. After optimization of VIGS, *MgCYC1*-TRV2, *MgCYC2*-TRV2, and *MgCYC1:MgCYC2*-TRV2 were used to electroporate EHA105 as described.

SEEDLING INOCULATION WITH VIGS CONSTRUCTS

Mimulus guttatus seedlings were grown to the two to three leaf pair stage at 20°C–22°C under long-day (16 hr. light/8 hr. dark) conditions on a 1:1 mix of vermiculite and soil. One hundred to 200 seedlings were inoculated with a 1:1 ratio of *Agrobacterium tumefaciens* GV3101 or EHA105 carrying TRV1 and *MgPDS*-TRV2, or Empty-TRV2 per treatment as previously described (Hileman et al., 2005). Batches of 50 *M. guttatus* PR and IM767 seedlings were subjected to four different inoculation treatments: 1 min. vacuum infiltration, 3 min. vacuum infiltration, 15 min. submersion without vacuum, and injection of leaves with a needleless syringe. Inoculated seedlings were replanted in soil and grown for an additional two (IM767) to four (PR) weeks at 20°C–22°C before leaf tissue was collected for RNA extraction. Differences in tissue harvest times were based on interpopulation variation in phenotype emergence. All surviving plants were examined for evidence of photobleaching as well as any obvious differences in flowering time and flower development relative to wild type. Once conditions had been optimized, VIGS was carried out as previously described in approximately 200 IM767 seedlings using the *MgCYC1*-TRV2, *MgCYC2*-

TRV2, or *MgCYC1:MgCYC2*-TRV2 construct with 1 min. vacuum infiltration.

RNA extraction and gene expression analysis

Leaf tissue from surviving plants was harvested and pooled per five to 10 individual plants, and total RNA was extracted using TriReagent (Applied Biosystems, Foster City, California). For each RNA pool, 1 μg was reverse transcribed using the iScript cDNA Synthesis Kit (Bio-Rad). cDNA was diluted 1:10 and 2 μL was used as a PCR template to screen for the presence of TRV2 and TRV1 plasmids as previously described (Hileman et al., 2005). After identification of infected pools, total RNA was extracted from leaves of individual plants. cDNA was then synthesized after DNA digestion with TURBO DNA-free (Applied Biosystems), and each cDNA was screened for presence of TRV2 and TRV1. *ACTIN* was amplified for 28 cycles as an internal control as described in Prasad et al. (2001).

To determine if a reduction in *PDS* levels was correlated with photobleaching, a ca. 150 bp region of *PDS* was amplified from cDNA of green leaf RNA harvested from Empty-TRV2-infected and uninfected individuals, and white leaf RNA harvested from *MgPDS*-TRV2-infected individuals. MgPDSrt-F (5′-CGAAGATGGCATTTTTGGAT-3′) and MgPDSrt-R (5′-ATGGCATCTCTTTCCATTCG-3′) were designed in Primer3 (Rozen & Skaletsky, 2000) to amplify a region downstream of the VIGS *PDS* insert region, and PCRs were run for 28, 30, and 32 cycles to confirm linearity. *MgPDS* expression levels were normalized against *ACTIN* in ImageJ (Abramoff et al., 2004) with two to six biological replicates.

Silencing of *MgCYC1* and *MgCYC2* was determined using quantitative (q) reverse transcriptase (RT)-PCR. The *MgCYC1* primers MgCYC1.rt.new.F (5′-CGAACAACGGGAAATTATGC-3′) and MgCYC1.rt.new.R (5′-GCCGTAGTTGGAACTCGAAA-3′), and the *MgCYC2* primers MgCYC2.rt.new.F (5′-CGGCCCGTCTGCTAATAAT-3′) and MgCYC2.rt.new.R (5′-CCTATTGATGAACTTGGCTGGT-3′) were designed to amplify a 150 bp fragment downstream of the VIGS construct sequence in Primer3 (Rozen & Skaletsky, 2000). Primer efficiency was determined using Fast SYBR Green Master Mix (Life Technologies) as previously described (Preston & Hileman, 2010). After correcting for transcriptional stability, cycle threshold values were normalized against the housekeeping gene *EF1alpha* as previously described (Scoville et al., 2011), and the mean was calculated for four technical replicates. Flowers positive for *MgCYC1*-TRV2, *MgCYC2*-TRV2, and *MgCYC1:MgCYC2*-TRV2 were examined for organ number, shape, and identity, and compared to wild type flowers.

Results and Discussion

Photobleaching in MgPDS-TRV2 VIGS treated plants

Silencing of *PDS* causes a characteristic photobleached phenotype that can be easily screened by the naked eye (Benedito et al., 2004; Hileman et al., 2005). To compare the efficiency of VIGS for the two populations of *Mimulus guttatus*, we attempted to infect plants with two *Agrobacterium tumefaciens* strains, using four different treatments. Each *MgPDS*-TRV2-treated plant was then screened for evidence of photobleaching. For the PR population, *MgPDS*-TRV2-treated seedling survival ranged from 68% to 84% using GV3101 and 3% to 29% using EHA105, with the highest survival rate for the 3 min. vacuum infiltration treatment for both *A. tumefaciens* strains (Table 1). Photobleached plants were identified in all but the leaf injection treatment for both GV3101 and EHA105. For the three successful treatments using GV3101 (1%–6%), the percentage of photobleached survivors was significantly higher (6%) after 3 min. vacuum infiltration (Table 1). This trend was also observed using EHA105. However, treatments using EHA105 were less efficient (0%–3% infected) than GV3101 (Table 1). Furthermore, for all plants showing a phenotype, photobleaching was only observed on one or two leaves (Fig. 2A, B); no photobleaching was observed in reproductive tissues.

Similar to the PR population, no photobleaching was observed for the leaf injection treatment in IM767. Furthermore, unlike the PR population, IM767 seedlings were unable to survive 3 min. vacuum infiltration regardless of the *Agrobacterium* strain used. For the other two treatments, survival ranged from 25% (1 min. vacuum; EHA105) to 40% (15 min. dip; both *Agrobacterium* strains). However, photobleached individuals were only found after 1 min. vacuum infiltration. The efficiency of *MgPDS*-TRV2 VIGS using GV3101 (3%) was similar to the most efficient treatments in the PR population. By contrast, 1 min. vacuum infiltration using EHA105 was significantly higher in the IM767 population (24%) versus the PR population (Table 1). This level of VIGS efficiency is similar to that found for *PDS* silencing in *Papaver* L. using EHA105 (Hileman et al., 2005) and *Aquilegia* L. using GV3101 (Gould & Kramer, 2007); VIGS has been successfully used in both these species to elucidate the function of flower developmental genes (Drea et al., 2007; Kramer et al., 2007; Yellina et al., 2010; Hands et al., 2011).

Table 1. Survival and infection rates for VIGS-treated *Mimulus guttatus* DC. seedlings.

	Point Reyes				Iron Mountain 767			
Agrobacterium strain	1 min.	3 min.	3 min.	15 min.	1 min.	1 min.	3 min.	15 min.
GV3101								
Construct	PDS	E	PDS	PDS	E	PDS	PDS	PDS
N treated	150	100	100	200	100	100	100	100
Survival (%)	68	60	84	67	40	34	0	40
Survivors infected (%)	2	0	6	1	0	3	N/A	0
Phenotype[1] (%)	2	0	6	1	0	3	N/A	0
EHA105								
Construct	PDS	E	PDS	PDS	E	PDS	PDS	PDS
N treated	150	100	100	150	100	150	100	100
Survival (%)	3	24	29	24	21	25	0	40
Survivors infected (%)	0	0	3	0	14	24	N/A	0
Phenotype[1] (%)	0	0	3	0	0	24	N/A	0

Abbreviations: PDS, *MgPDS*-TRV2; E, Empty-TRV2.
[1] Percentage of survivors.

Furthermore, ca. 50% of the IM767 plants showing a phenotype were almost completely photobleached (Fig. 2D, E). This level of photobleaching caused severe retardation (Fig. 2D, E), followed by death prior to development of the reproductive organs. Consequently, no photobleaching was observed in reproductive structures.

To confirm that photobleaching in both *Mimulus guttatus* populations was positively correlated with *MgPDS*-TRV2 and TRV1 infection, and was not a result of infection per se, tissues from both *MgPDS*-TRV2- and Empty-TRV2-treated plants were PCR screened for the presence of TRV2 and TRV1. For both the PR and IM767 populations, all photobleached leaves were infected with both *MgPDS*-TRV2 and TRV1 (Fig. 3A); no green leaves were positive for either vector. Control plants positive for both Empty-TRV2 and TRV1 were only found in the IM767 population using EHA105 (14%), consistent with infection rates for *MgPDS*-TRV2 (Table 1; Fig. 3A). None of these infected control plants showed photobleaching in vegetative or reproductive tissues, and growth was normal throughout development. Thus, photobleaching was correlated with *MgPDS*-TRV2 infection, rather than viral infection per se. Furthermore, all Empty-TRV2-treated plants that screened positive for the virus in leaves also screened positive in flowers, suggesting that infection remains into the reproductive stage of development.

PDS TRANSCRIPT LEVELS IN PHOTOBLEACHED *MIMULUS GUTTATUS* PLANTS

To verify that photobleaching in *MgPDS*-TRV2-infected plants correlated with reduced endogenous *MgPDS* transcript levels, we performed RT-PCR on both PR and IM767 plants infected with *MgPDS*-TRV2 in GV3101 and EHA105, IM767 plants infected with Empty-TRV2 in EHA105, and plants from the same treatments that were not infected. For each infected plant, endogenous *MgPDS* expression levels were calculated relative to uninfected plants from the same treatment (set to an expression level of 1) after standardization against *ACTIN* (Fig. 3B). RT-PCR analyses confirmed silencing of endogenous *MgPDS* in *MgPDS*-TRV2 plants relative to both uninfected and Empty-TRV2 control plants (Fig. 3B). For both GV3101 and EHA105 treatments, average silencing was two-fold with a high level of variation between individuals, ranging from no significant silencing to 10-fold silencing (Fig. 3B). Because whole leaves were harvested for expression analyses, inter-individual variation in endogenous *MgPDS* expression is most likely due to differences in the number of leaf cells infected with *MgPDS*-TRV2. The amount of photobleaching per *MgPDS*-TRV2-infected individual ranged from small sectors on individual leaves (GV3101 in PR) to complete photobleaching of one or two leaves (EHA105 in PR and IM767) to almost complete photobleaching of the whole seedling (EHA105 and GV3101 in IM767) (Fig. 2A, B, D, E). This level of VIGS photobleaching variation is consistent with reports from other species (Hileman et al., 2005; Liu & Page, 2008).

TRANSCRIPT SILENCING OF PUTATIVE FLORAL *CYC* SYMMETRY GENES

The fact that *Mimulus guttatus* IM767 infection persists into flowers (previous section) suggests efficacy of VIGS in reproductive tissues. However, in order to verify that infection of reproductive tissues

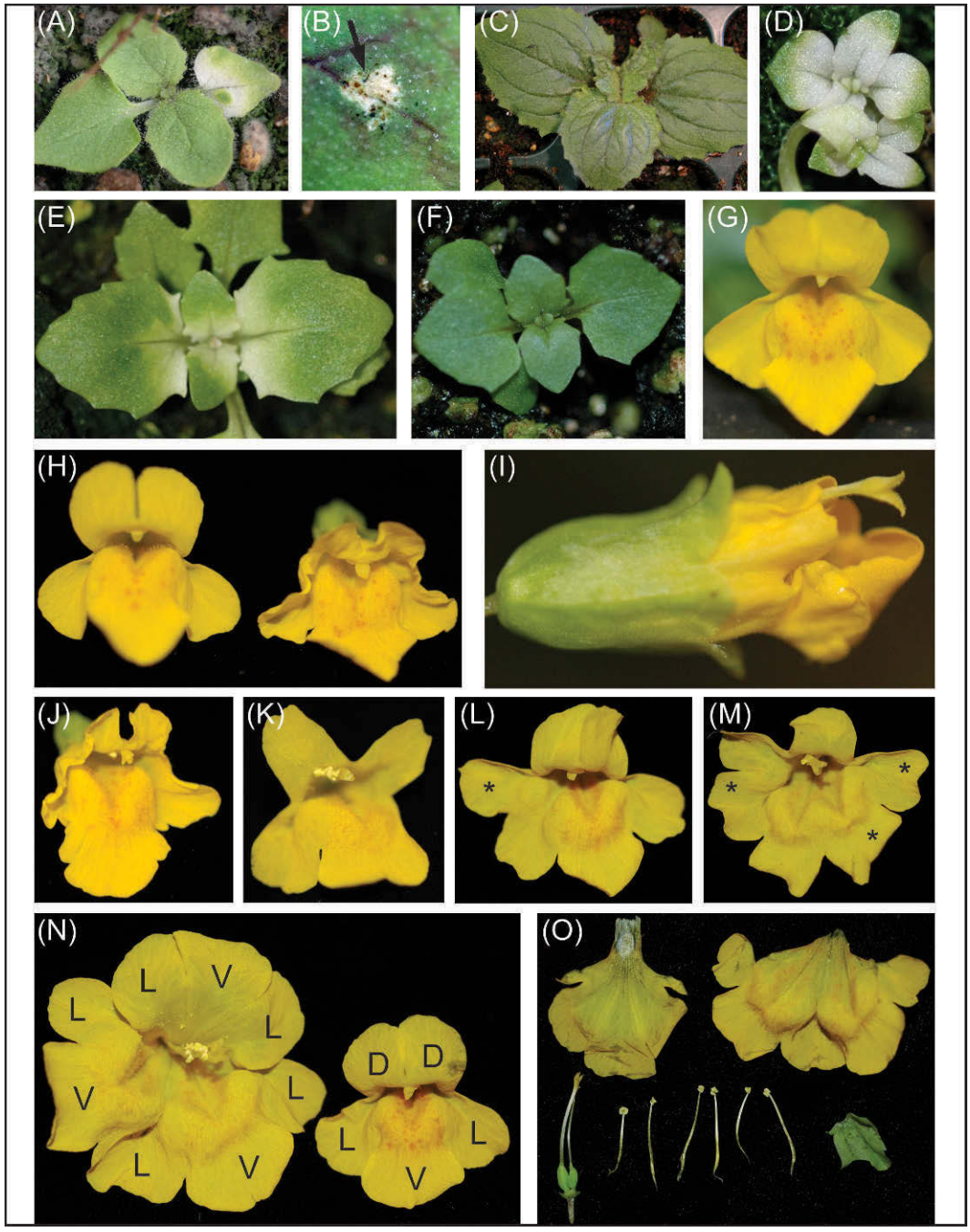

Figure 2. Variation in leaf photobleaching and flower morphology for *MgPDS*-TRV2- and *MgCYC*-TRV2-infected plants. A, B. Infected plants of *Mimulus guttatus* PR treated with *MgPDS*-TRV2 in GV3101 show variation in the extent of photobleaching [arrow in (B)] in individual leaves. —C. Uninfected *M. guttatus* PR plants treated with *MgPDS*-TRV2 show no sign of photobleaching. —D. Almost completely photobleached *MgPDS*-TRV2 in EHA105-infected *M. guttatus* IM767 seedling. —E. Initial stages of systemic photobleaching for an *MgPDS*-TRV2 in GV3101-infected *M. guttatus* IM767 seedling. —F. Uninfected *M. guttatus* IM767 plants treated with *MgPDS*-TRV2 show no sign of photobleaching. —G. Empty-TRV2 positive flower showing wild type morphology. —H. *MgCYC1*-TRV2-infected flowers (right) have small dorsal petal and wavy petal margins compared to uninfected flowers (left). —I. Infected flower in H. Infected flower prior to anthesis has shortened dorsal petals, resulting in protrusion of the stigma. —J. Another example of an *MgCYC1*-TRV2-infected flower showing wavy margins in all petals. K–M. *MgCYC1:MgCYC2*-TRV2-infected flowers have an abnormal number of lateral and/or ventral

also causes gene silencing and has a correlated effect on phenotype, we silenced two homologs of the *Antirrhinum majus* clade II TCP family flower symmetry genes *CYCLOIDEA* (*CYC*) and *DICHOTOMA* (*DICH*) (Luo et al., 1996, 1999). In *A. majus*, mutations in *CYC* result in partial loss of dorsal petal and staminode identity, resulting in plants with five fully developed stamens and partially radialized petals (Luo et al., 1996, 1999). By contrast, the *dich* mutant has no effect on stamen number but causes the loss of internal asymmetry within the dorsal petals; loss-of-function mutations in both *CYC* and *DICH* result in fully radialized flowers that have six ventral petals and six ventral stamens (Luo et al., 1996, 1999).

Of the IM767 seedlings vacuum infiltrated for 1 min. with the *MgCYC* gene-silencing constructs, three (6% of survivors), five (28% of survivors), and six (15% of survivors) individuals had flowers that were positive for *MgCYC1*-TRV2, *MgCYC2*-TRV2, and *MgCYC1:MgCYC2*-TRV2, respectively. Q-RT-PCR analyses of gene expression revealed that *MgCYC1* expression was significantly reduced in *MgCYC1*-TRV2 and *MgCYC1:MgCYC2*-TRV2-infected versus uninfected flowers collected for RNA post-anthesis (Fig. 3C). Similarly, *MgCYC2* expression was significantly reduced in *MgCYC2*-TRV2 and *MgCYC1:MgCYC2*-TRV2-infected versus uninfected post-anthesis flowers (Fig. 3C). This demonstrates that gene silencing was target specific. In the case of *MgCYC2*-silenced flowers, no abnormal phenotype was detected relative to uninfected plants in terms of organ number, size, shape, or identity. By contrast, infection and partial silencing of *MgCYC1*, and *MgCYC1* and *MgCYC2* together was correlated with abnormal petal and/or stamen whorl phenotypes but did not affect sepal morphology (Fig. 2H–O).

All nine *MgCYC1*-TRV2-infected flowers from three plants had petals with wavy margins compared to the smooth margins of wild type and Empty-TRV2-infected flowers (Fig. 2G–J). In each case, this growth defect was found in dorsal, lateral, and ventral petals (Fig. 2H–J). In addition to wavy petal margins, the two dorsal petals of infected flowers appeared shortened relative to wild type dorsal petals and infected lateroventral petals (Fig. 2H–J). Quantitative analyses of flower size revealed that *MgCYC1*-TRV2-infected flowers were shorter and narrower than uninfected flowers (Fig. 3D, E). Furthermore, the average ratio between dorsal and ventral petal lobe length was smaller in *MgCYC1*-TRV2-infected relative to uninfected flowers (Fig. 3F). This suggests that the reduction in growth was more extreme for dorsal petals than for ventral petals. Indeed, in some cases, reduction of dorsal petal size was evident at the bud stage (Fig. 2I); in wild type flower buds, the dorsal petals enclose the reproductive structures, whereas in two *MgCYC1*-TRV2-infected flowers, the anthers and stigma protruded from the flower bud.

In striking contrast to *MgCYC1*- and *MgCYC2*-silenced flowers, all *MgCYC1:MgCYC2*-TRV2-infected flowers had extra petals and/or stamens relative to wild type and Empty-TRV2-infected flowers (Figs. 2L–O, 3G). In wild type *Mimulus guttatus* plants, five stamen primordia give rise to two lateral and two ventral stamens and a single dorsal staminode that arrests growth in early development (pers. obs.). By contrast, in *MgCYC1:MgCYC2*-TRV2-infected flowers, one or two stamens developed in the dorsal region, resulting in a total of five to six pollen-producing stamens at anthesis (Figs. 2M, 3G). This gene-silenced phenotype is similar to *cyc* and *cyc:dich* mutants of *Antirrhinum majus*, which develop five and six stamens, respectively, compared to four stamens and one dorsal staminode of wild type flowers (Luo et al., 1996, 1999). In addition to stamens, *MgCYC1:MgCYC2*-TRV2-infected flowers showed organ number and identity defects in the petal whorl. Infected flowers ranged from having one less lateral petal to having both extra lateral and ventral petals (Figs. 2K–O, 3G). In the most extreme case, flowers were almost fully radialized due to the development of three sets of two lateral and one ventral petal. The flowers of this plant also had six stamens and showed a novel phenotype consisting of two instead of one gynoecium (Fig. 2N, O).

DIVERGENCE OF *CYC* GENE FUNCTION IN ASTERIDS

MgCYC1 and *MgCYC2* are the closest homologs of *CYC* and *DICH* from *Antirrhinum majus*, falling into the ECE CYC2 clade of TCP genes (Howarth & Donoghue, 2006). However, the duplication events that gave rise to the ECE CYC2 clade paralogs of *Mimulus guttatus* and *A. majus* occurred independently. Thus, comparison of these genes in asterids can inform our understanding of functional diversification after gene duplication. The VIGS data

←
petals (asterisks). —N. Comparison of an extreme *MgCYC1:MgCYC2*-TRV2-silenced floral phenotype (left) with that of an uninfected flower (right). —O. Dissected flower from (N) showing an increase in stamen, petal, and gynoecium number. In addition to a doubling of the lateroventral petal unit in the ventral domain, the dorsal petals are partially transformed into a dorsal lateroventral-like unit. D, dorsal; L, lateral; V, ventral.

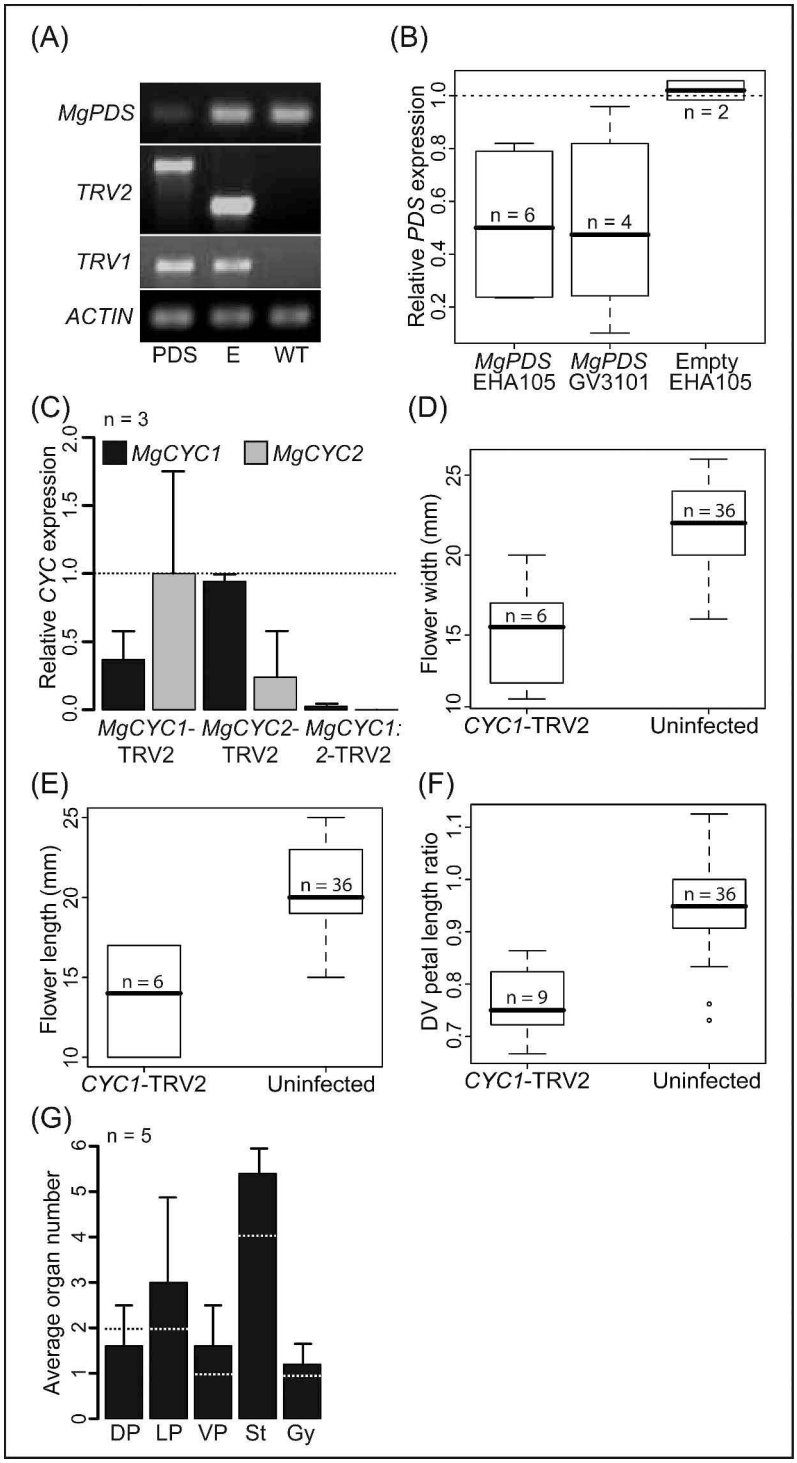

Figure 3. VIGS-mediated silencing of *PDS* and *CYC* genes. —A. RT-PCR showing the presence of TRV vectors in two representative IM767 individuals infected with *MgPDS*-TRV2 (*PDS*; larger TRV2 band) and Empty-TRV2 (E; smaller TRV2 band). These screening methods were used to determine the number of infected individuals described in Table 1. Endogenous levels of *MgPDS* are reduced in individuals infected with *MgPDS*-TRV2 relative to Empty-TRV2-infected and uninfected individuals. *ACTIN* was amplified as an internal control. —B. Boxplots showing variation in *ACTIN*-standardized endogenous *MgPDS* expression levels relative to the average of two to four uninfected individuals (dotted line) for each population and

presented in this paper support both similar and divergent functions for *MgCYC1* and *MgCYC2* in flower development and suggest differential sub- and neo-functionalization of paralogous genes after independent duplications in Plantaginaceae (*A. majus*) and Phrymaceae (*M. guttatus*).

In the case of *MgCYC1*, silencing has an effect on dorsal petal size, consistent with the known function of TCP genes on dorsal petal development and cell proliferation (Luo et al., 1996, 1999; Feng et al., 2006; Busch & Zachgo, 2007; Broholm et al., 2008; Preston & Hileman, 2009; Kieffer et al., 2011; Bai et al., 2012; Braun et al., 2012). However, within the ECE CYC2 clade, the specific phenotype observed in *MgCYC1*-silenced flowers is unique to *Mimulus guttatus*. In *Antirrhinum majus*, mutations in either *CYC* or *DICH* have negative effects on dorsal petal growth, but mutations in *CYC* have positive effects on stamen growth. Furthermore, lateral petals of double *cyc:dich* mutants are transformed into ventral petals, and both petal and stamen number is increased (Luo et al., 1996, 1999). A role in dorsal identity is also suggested for species in the Commelinaceae, Poaceae, Malpighiaceae, Caprifoliaceae, Gesneriaceae, and Papaveraceae based on gene expression data (Damerval et al., 2007; Song et al., 2009; Yuan et al., 2009; Zhang et al., 2010; Howarth et al., 2011; Preston & Hileman, 2012).

Similar to *Antirrhinum majus cyc* mutants, silencing of *MgCYC1* negatively affects dorsal petal growth. However, like *A. majus dich* mutants, *Mimulus guttatus* dorsal petals are not transformed into lateral or ventral petals, and there is no effect on floral organ number. *MgCYC1* silencing also causes growth defects at the margins of dorsal, lateral, and ventral petals; this phenotype is so far novel to loss-of-function ECE CYC2 clade genes. Interestingly, a similar phenotype was recently observed when several distantly related *CINCINATTA*-like (*CIN*-like) TCP genes were simultaneously silenced (Koyama et al., 2011). Given the lack of this phenotype in Plantaginaceae and Asteraceae *CYC*-like mutant backgrounds, it is most parsimonious to infer the recent acquisition of petal margin growth function in the *MgCYC1* lineage. However, it is unclear why this phenotype was not observed in *MgCYC1:MgCYC2*-TRV2-infected plants. Our working hypothesis is that the loss of competition between *MgCYC1* and *MgCYC2* for protein partners may have resulted in a gain of function phenotype; this remains to be tested.

Although silencing of *MgCYC2* in a few *Mimulus guttatus* flowers resulted in no abnormal phenotypes, the observation that double *MgCYC1:MgCYC2*-TRV2-infected flowers on average had more petals and stamens than single gene-silenced flowers suggests that *MgCYC1* and *MgCYC2* have a redundant role in specifying dorsal identity and stabilizing organ number. A similar role has been assigned to *CYC* and *DICH* and is suggested for other asterid *CYC*-like genes (Luo et al., 1996, 1999; Cubas et al., 1999; Gao et al., 2008; Song et al., 2009; Preston et al., 2009, 2011; Fambrini et al., 2011). However, the fact that *MgCYC1:MgCYC2*-TRV2-infected flowers tend to duplicate the lateroventral petals as a single unit tentatively suggests differential integration of the petal module in asterids. This hypothesis warrants further investigation in the future.

Conclusion

By applying different treatments to two ecologically and morphologically distinct populations, we have optimized VIGS as a reverse genetics tool to assay protein function in *Mimulus guttatus*. Specifically, *Agrobacterium tumefaciens* EHA105-mediated treatments of IM767 seedlings at the two to three leaf pair stage, via 1 min. vacuum infiltration, proved highly efficient. This treatment of IM767 seedlings yielded ca. 14%–24% infected survivors, the majority of which carried the virus in all tissues throughout development (Table 1). In the case of infection with *MgPDS*-TRV2, systemic infection caused severe photobleaching, resulting in death prior to flowering. Thus, it was not possible to determine the ability of the virus to infect reproductive tissues. By contrast,

←
treatment. Endogenous *MgPDS* levels are reduced in *MgPDS*-TRV2-infected individuals, but not Empty-TRV2-infected controls, relative to uninfected individuals using both EHA105 and GV3101 *Agrobacterium* strains. Data for *MgPDS*-TRV2-infected individuals include both the PR and IM767 populations; Empty-TRV2-infected individuals are from the IM767 population only. Solid horizontal line, median; box, interquartile range; whiskers, extending to the further point that is within 1.5× the interquartile range from the box. —C. Quantitative-RT-PCR expression data for *MgCYC1* (black bars) and *MgCYC2* (gray bars) in uninfected and *MgCYC1:MgCYC2*-TRV2-infected flowers post-anthesis. Data are averages for three biological replicates. Error bars denote standard deviations. —D. Effect of *CYC1* silencing on flower width. —E. Effect of *CYC1* silencing on flower height. —F. Effect of *CYC1* silencing on the ratio of dorsal to ventral (DV) petal lobe length. —G. Effect of simultaneous *CYC1* and *CYC2* silencing on organ number. Lateral petal (LP), ventral petal (VP), stamen (St), and gynoecium (Gy), but not dorsal petal (DP), numbers are all increased relative to uninfected control plants (dotted line). Error bars denote standard deviations.

screening for both TRV2 and TRV1 in individuals infected with the Empty-TRV2 control vector revealed 100% retention of the virus in flowers, without any effect on flowering time, vegetative and inflorescence development, or seed set. The efficacy of VIGS in flowers was verified by the silencing of two *CYC*-like homologs, resulting in wavy petal margins, reduced dorsal petal growth, extra lateroventral petals and stamens, and variable loss of dorsal identity. Together, these data demonstrate the potential of VIGS as a fast and reliable method to assay gene function in *M. guttatus*, advancing this species further as a tool for addressing fundamental ecological and evolutionary questions.

Literature Cited

Abramoff, M. D., P. J. Magelhães & S. J. Ram. 2004. Image processing with ImageJ. Biophotonics Int. 11: 36–42.

Allen, W. R. & P. M. Sheppard. 1971. Copper tolerance in some Californian populations of the monkey flower, *Mimulus guttatus*. Proc. Roy. Soc. London, Ser. B, Biol. Sci. 177: 177–196.

Angert, A. L. & D. W. Schemske. 2005. The evolution of species' distributions: Reciprocal transplants across the elevation ranges of *Mimulus cardinalis* and *M. lewisii*. Evolution 59: 1671–1684.

Bai, F., R. Reinheimer, D. Durantini, E. A. Kellogg & R. J. Schmidt. 2012. TCP transcription factor, *BRANCH ANGLE DEFECTIVE 1* (*BAD1*), is required for normal tassel branch angle formation in maize. Proc. Natl. Acad. Sci. U.S.A. PMID: 22773815.

Baulcombe, D. C. 1999. Fast forward genetics based on virus-induced gene silencing. Curr. Opin. Pl. Biol. 2: 109–113.

Beardsley, P. M. & R. G. Olmstead. 2002. Redefining Phrymaceae: The placement of *Mimulus*, tribe Mimuleae, and *Phryma*. Amer. J. Bot. 89: 1093–1102.

Beardsley, P. M., S. E. Schoenig, J. B. Whittall & R. G. Olmstead. 2004. Patterns of evolution in Western North American *Mimulus* (Phrymaceae). Amer. J. Bot. 91: 474–489.

Benedito, V. A., P. B. Visser, G. C. Angenent & F. A. Krens. 2004. The potential of virus-induced gene silencing for speeding up functional characterization of plant genes. Genet. Molec. Res. 3: 323–341.

Bradshaw, H. D. & D. W. Schemske. 2003. Allele substitution at a flower colour locus produces a pollinator shift in monkey-flowers. Nature 426: 176–178.

Braun, N., A. de Saint Germain, J. P. Pillot, S. Boutet-Mercey, M. Dalmais, I. Antoniadi, X. Li, A. Maia-Grondard, C. Le Signor, N. Bouteiller, D. Luo, A. Bendahmane, C. Turnbull & C. Rameau. 2012. The pea TCP transcription factor *PsBRC1* acts downstream of *Strigolactones* to control shoot branching. Pl. Physiol. (Lancaster) 158: 225–238.

Broholm, S. K., S. Tahtiharju, R. A. Laitinen, V. A. Albert, T. H. Teeri & P. Elomaa. 2008. A TCP domain transcription factor controls flower type specification along the radial axis of the *Gerbera* (Asteraceae) inflorescence. Proc. Natl. Acad. Sci. U.S.A. 105: 9117–9122.

Burch-Smith, T. M., M. Schiff, Y. Liu & S. P. Dinesh-Kumar. 2006. Efficient virus-induced gene silencing in *Arabidopsis*. Pl. Physiol. 142: 21–27.

Busch, A. & S. Zachgo. 2007. Control of corolla monosymmetry in the Brassicaceae *Iberis amara*. Proc. Natl. Acad. Sci. U.S.A. 104: 16714–16719.

Cooley, A. M. & J. H. Willis. 2009. Genetic divergence causes parallel evolution of flower color in Chilean *Mimulus*. New Phytol. 183: 729–739.

Cubas, P., C. Vincent & E. Coen. 1999. An epigenetic mutation responsible for natural variation in floral symmetry. Nature 401: 157–161.

Damerval, C., M. Le Guilloux, M. Jager & C. Charon. 2007. Diversity and evolution of *CYCLOIDEA*-like TCP genes in relation to flower development in Papaveraceae. Pl. Physiol. 143: 759–772.

Demircan, T. & M. S. Akkaya. 2010. Virus induced gene silencing in *Brachypodium distachyon*, a model organism for cereals. Pl. Cell Tissue Organ Cult. 100: 91–96.

Demmig-Adams, B. & W. W. Adams. 1992. Photoprotection and other responses of plants to high light stress. Annual Rev. Pl. Physiol. Pl. Molec. Biol. 43: 599–626.

Di Stilio, V. S. 2011. Empowering plant evo-devo: Virus induced gene silencing validates new and emerging model systems. Bioessays 33: 711–718.

Di Stilio, V. S., R. A. Kumar, A. M. Oddone, T. R. Tolkin, P. Salles & K. McCarthy. 2010. Virus-induced gene silencing as a tool for comparative functional studies in *Thalictrum*. PLoS ONE 5: 12,064.

Dinesh-Kumar, S. P., R. Anandalakshmi, R. Marathe, M. Schiff & Y. Liu. 2003. Virus-induced gene silencing. Meth. Molec. Biol. 236: 287–294.

Drea, S., L. C. Hileman, G. de Martino & V. F. Irish. 2007. Functional analyses of genetic pathways controlling petal specification in poppy. Development 134: 4157–4166.

Fagard, M. & H. Vaucheret. 2000. Systemic silencing signal(s). Pl. Molec. Biol. 43: 285–293.

Fambrini, M., M. Salvini & C. Pugliesi. 2011. A transposon-mediate inactivation of a *CYCLOIDEA*-like gene originates polysymmetric and androgynous ray flowers in *Helianthus annuus*. Genetica 139: 1521–1529.

Feng, X., Z. Zhao, Z. Tian, S. Xu, Y. Luo, Z. Cai, Y. Wang, J. Yang, Z. Wang, J. Chen, L. Zheng, X. Guo, J. Luo, S. Sato, S. Tabata, W. Ma, X. Cao, X. Hu, C. Sun & D. Luo. 2006. Control of petal shape and floral zygomorphy in *Lotus japonica*. Proc. Natl. Acad. Sci. U.S.A. 103: 4970–4975.

Fishman, L., A. J. Kelly & J. H. Willis. 2002. Minor quantitative trait loci underlie floral traits associated with mating system divergence in *Mimulus*. Evolution 56: 2138–2155.

Gao, Q., J. H. Tao, D. Yan, Y. Z. Wang & Z. Y. Li. 2008. Expression differentiation of *CYC*-like floral symmetry genes correlated with their protein sequence divergence in *Chirita heterotricha* (Gesneriaceae). Developm. Genes Evol. 218: 341–351.

Gould, B. & E. M. Kramer. 2007. Virus-induced gene silencing as a tool for functional analysis in the emerging model plant *Aquilegia* (columbine, Ranunculaceae). Pl. Meth. 3: 6.

Grønlund, M., G. Constantin, E. Piednoir, J. Kovacev, I. E. Johansen & O. S. Lund. 2008. Virus-induced gene silencing in *Medicago truncatula* and *Lathyrus odorata*. Virus Res. 135: 345–349.

Hall, M. C. & J. H. Willis. 2005. Transmission ratio distortion in intraspecific hybrids of *Mimulus guttatus*:

Implications for genomic divergence. Genetics 170: 375–386.

Hall, M. C. & J. H. Willis. 2006. Divergent selection on flowering time contributes to local adaptation in *Mimulus guttatus* populations. Evolution 60: 2466–2477.

Hamilton, A. J. & D. C. Baulcombe. 1999. A species of small antisense RNA in posttranscriptional gene silencing in plants. Science 286: 950–952.

Hammond, S. M., E. Bernstein, D. Beach & G. J. Hannon. 2000. An RNA-directed nuclease mediates post-transcriptional gene silencing in *Drosophila* cells. Nature 404: 293–296.

Hands, P., N. Vosnakis, D. Betts, V. F. Irish & S. Drea. 2011. Alternate transcripts of a floral developmental regulator have both distinct and redundant functions in opium poppy. Ann. Bot. (Oxford) 107: 1557–1566.

Hileman, L. C., S. Drea, G. Martino, A. Litt & V. F. Irish. 2005. Virus-induced gene silencing is an effective tool for assaying gene function in the basal eudicot species *Papaver somniferum* (opium poppy). Pl. J. 44: 334–341.

Holeski, L. M. & J. K. Kelly. 2006. Mating system and the evolution of quantitative traits: An experimental study of *Mimulus guttatus*. Evolution 60: 711–723.

Holzberg, S., P. Brosio, C. Gross & G. P. Pogue. 2002. Barley stripe mosaic virus-induced gene silencing in a monocot plant. Pl. J. 30: 315–327.

Howarth, D. G. & M. J. Donoghue. 2006. Phylogenetic analysis of the "ECE" (*CYC/TB1*) clade reveals duplications predating the core eudicots. Proc. Natl. Acad. Sci. U.S.A. 103: 9101–9106.

Howarth, D. G., T. Martins, E. Chimney & M. J. Donoghue. 2011. Diversification of *CYCLOIDEA* expression in the evolution of bilateral flower symmetry in Caprifoliaceae and Lonicera (Dipsacales). Ann. Bot. (Oxford) 107: 1521–1532.

Igarashi, A., K. Yamagata, T. Sugai, Y. Takahashi, E. Sugawara, A. Tamura, H. Yaegashi, N. Yamagishi, T. Takahashi, M. Isogai, H. Takahashi & N. Yoshikawa. 2009. Apple latent spherical virus vectors for reliable and effective virus-induced gene silencing among a broad range of plants including tobacco, tomato, *Arabidopsis thaliana*, cucurbits, and legumes. Virology 386: 407–416.

Ivey, C. T., D. E. Carr & M. D. Eubanks. 2009. Genetic variation and constraints on the evolution of defense against spittlebug (*Philaenus spumarius*) herbivory in *Mimulus guttatus*. Heredity 102: 303–311.

Kelly, A. J. & J. H. Willis. 1998. Polymorphic microsatellite loci in *Mimulus guttatus* and related species. Molec. Ecol. 7: 769–774.

Kieffer, M., V. Master, R. Waites & B. Davies. 2011. *TCP14* and *TCP15* affect internode length and leaf shape in *Arabidopsis*. Pl. J. 68: 147–158.

Koyama, T., M. Ohme-Takagi & F. Sato. 2011. Generation of serrated and wavy petals by inhibition of the activity of TCP transcription factors in *Arabidopsis thaliana*. Pl. Signal Behav. 6: 697–699.

Kramer, E. M., L. Holappa, B. Gould, M. A. Jaramillo, D. Setnikov & P. M. Santiago. 2007. Elaboration of B gene function to include the identity of novel floral organs in the lower eudicot *Aquilegia*. Pl. Cell 19: 750–766.

Kumagai, M. H., J. Donson, G. Della-Cioppa, D. Harvey, K. Hanley & L. K. Grill. 1995. Cytoplasmic inhibition of carotenoid biosynthesis with virus-derived RNA. Proc. Natl. Acad. Sci. U.S.A. 92: 1679–1683.

Liu, E. & J. E. Page. 2008. Optimized cDNA libraries for virus-induced gene silencing (VIGS) using tobacco rattle virus. Pl. Meth. 4: 5.

Liu, Y., M. Schiff & S. P. Dinesh-Kumar. 2002. Virus-induced gene silencing in tomato. Pl. J. 34: 777–786.

Lowry, D. B., M. C. Hall, D. E. Salt & J. H. Willis. 2009. Genetic and physiological basis of adaptive salt tolerance divergence between coastal and inland *Mimulus guttatus*. New Phytol. 183: 776–788.

Lu, H.-C., H.-H. Chen, W.-C. Tsai, W.-H. Chen, H.-J. Su, D. C.-N. Chang & H.-H. Yeh. 2007. Strategies for functional validation of genes involved in reproductive stages of orchids. Pl. Physiol. 143: 558–569.

Luo, D., R. Carpenter, C. Vincent, L. Copsey & E. Coen. 1996. Origin of floral asymmetry in *Antirrhinum*. Nature 383: 794–799.

Luo, D., R. Carpenter, L. Copsey, C. Vincent, J. Clark & E. Coen. 1999. Control of organ asymmetry in flowers of *Antirrhinum*. Cell 99: 367–376.

Pflieger, S., S. Blanchet, L. Camborde, G. Drugeon, A. Rousseau, M. Noizet, S. Planchais & I. Jupin. 2008. Efficient virus-induced gene silencing in *Arabidopsis* using a 'one-step' TYMV-derived vector. Pl. J. 56: 678–690.

Prasad, K., P. Sriram, C. S. Kumar, K. Kushalappa & U. Vijayraghavan. 2001. Ectopic expression of rice Os-MADS1 reveals a role in specifying the lemma and palea, grass floral organs analogous to sepals. Developm. Genes Evol. 211: 281–290.

Preston, J. C. & L. C. Hileman. 2009. Developmental genetics of floral symmetry evolution. Trends Pl. Sci. 14: 147–154.

Preston, J. C. & L. C. Hileman. 2010. SQUAMOSA-PROMOTER BINDING PROTEIN1 initiates flowering in *Antirrhinum majus* through the activation of meristem identity genes. Pl. J. 62: 704–712.

Preston, J. C. & L. C. Hileman. 2012. Parallel evolution of TCP and B-class genes in Commelinaceae flower bilateral symmetry. EvoDevo 3: 6.

Preston, J. C., M. A. Kost & L. C. Hileman. 2009. Conservation and diversification of the symmetry developmental program among close relatives of snapdragon with divergent floral morphologies. New Phytol. 182: 751–762.

Preston, J. C., C. C. Martinez & L. C. Hileman. 2011. Gradual disintegration of the floral symmetry gene network is implicated in the evolution of a wind-pollination syndrome. Proc. Natl. Acad. Sci. U.S.A. 108: 2343–2348.

Purkayastha, A. & I. Dasgupta. 2009. Virus-induced gene silencing: A versatile tool for discovery of gene functions in plants. Pl. Physiol. Biochem. (New Delhi) 47: 967–976.

Renner, T., J. Bragg, H. E. Driscoll, J. Cho, A. O. Jackson & C. D. Specht. 2009. Virus-induced gene silencing in the culinary ginger (*Zingiber officinale*): An effective mechanism for down-regulating gene expression in tropical monocots. Molec. Pl. 2: 1084–1094.

Robertson, D. 2004. VIGS vectors for gene silencing: Many targets, many tools. Annual Rev. Pl. Biol. 55: 495–519.

Rozen, S. & H. Skaletsky. 2000. Primer3 on the WWW for general users and for biologist programmers. Pp. 365–386 *in* S. Krawetz & S. Misener (editors), Bioinformatics Methods and Protocols: Methods in Molecular Biology. Humana Press, New Jersey.

Sather, D. N., M. Jovanovic & E. M. Golenberg. 2010. Functional analysis of B and C class floral organ genes in spinach demonstrates their role in sexual dimorphism. BMC Pl. Biol. 10: 46.

Scofield, S. R. & R. S. Nelson. 2009. Resources for virus-induced gene silencing in the grasses. Pl. Physiol. 149: 152–157.

Scofield, S. R., L. Huang, A. S. Brandt & B. S. Gill. 2005. Development of a virus-induced gene-silencing system for hexaploid wheat and its use in functional analysis of the *Lr21*-mediated leaf rust resistance pathway. Pl. Physiol. 138: 2165–2173.

Scoville, A. G., L. Barnett, S. Bodbyl-Roels, J. Kelly & L. C. Hileman. 2011. Differential regulation of a MYB transcription factor predicts transgenerational epigenetic inheritance of trichome density in *Mimulus guttatus*. New Phytol. 191: 251–263.

Song, C. F., Q. B. Lin, R. H. Liang & Y. Z. Wang. 2009. Expressions of ECE-CYC2 clade genes relating to abortion of both dorsal and ventral stamens in *Opithandra* (Gesneriaceae). BMC Evol. Biol. 9: 244.

Spitzer, B., M. M. Ben Zvi, M. Ovadis, E. Marhevka, O. Barkai, O. Edelbaum, I. Marton, T. Masci, M. Alon, S. Morin, I. Rogachev, A. Aharoni & A. Vainstein. 2007. Reverse genetics of floral scent: Application of tobacco rattle virus-based gene silencing in petunia. Pl. Physiol. 145: 1241–1250.

Sweigart, A. L. & J. H. Willis. 2003. Patterns of nucleotide diversity in two species of *Mimulus* are affected by mating system and asymmetric introgression. Evolution 57: 2490–2506.

Tai, Y. S., J. N. Bragg & M. C. Edwards. 2005. Virus vector gene silencing in wheat. BioTechniques 39: 310–314.

Vickery, R. K. 1978. Case studies in the evolution of species complexes in *Mimulus*. Evol. Biol. 11: 405–507.

Wege, S., A. Scholz, S. Gleissberg & A. Becker. 2007. Highly efficient virus-induced gene silencing (VIGS) in California poppy (*Eschscholzia californica*): An evaluation of VIGS as a strategy to obtain functional data from non-model plants. Ann. Bot. (Oxford) 100: 641–649.

Wu, C. A., D. B. Lowry, A. M. Cooley, K. M. Wright, Y. W. Lee & J. H. Willis. 2008. *Mimulus* is an emerging model system for the integration of ecological and genomic studies. Heredity 100: 220–230.

Wu, C. A., D. B. Lowry, L. I. Nutter & J. H. Willis. 2010. Natural variation for drought-response traits in the *Mimulus guttatus* species complex. Oecologia 162: 23–33.

Yellina, A. L., S. Orashakova, S. Lang, R. Erdmann, J. Leebens-Mack & A. Becker. 2010. Floral homeotic C function genes repress specific B function genes in the carpel whorl of the basal eudicot California poppy (*Eschscholzia californica*). EvoDevo 1: 13.

Yuan, Z., S. Gao, D. W. Xue, D. Luo, L. T. Li, S. Y. Ding, X. Yao, Z. A. Wilson, Z. Qian & D. B. Zhang. 2009. *RETARDED PALEA1* controls palea development and floral zygomorphy in rice. Pl. Physiol. 149: 235–244.

Zamore, P. D., T. Tuschl, P. A. Sharp & D. P. Bartel. 2000. RNAi: Double-stranded RNA directs the ATP-dependent cleavage of mRNA at 21 to 23 nucleotide intervals. Cell 101: 25–33.

Zhang, C., C. Yang, S. A. Whitham & J. H. Hill. 2009. Development and use of an efficient DNA-based viral gene silencing vector for soybean. Molec. Pl.-Microbe Interact. 22: 123–131.

Zhang, W., E. M. Kramer & C. C. Davis. 2010. Floral symmetry genes and the origin and maintenance of zygomorphy in a plant-pollinator mutualism. Proc. Natl. Acad. Sci. U.S.A. 107: 6388–6393.